Materials Science & Engineering A 649 (2016) 426–440

Contents lists available at ScienceDirect

Materials Science & Engineering A

journal homepage: www.elsevier.com/locate/msea

Multiaxial high cycle fatigue damage mechanisms associated with the different microstructural heterogeneities of cast aluminium alloys

Viet-Duc Le [a,b,c,*], Franck Morel [a], Daniel Bellett [a], Nicolas Saintier [b], Pierre Osmond [c]

[a] Arts et Métiers ParisTech, CER Angers – Laboratoire LAMPA – 2 Bd du Ronceray, 49035 Angers Cedex 1, France
[b] Arts et Métiers ParisTech, CER Bordeaux – Laboratoire I2M – Esplanade des Arts et Métiers, 33405 TALENCE Cedex, France
[c] PSA Peugeot Citroën, 18 rue des fauvelles, 92256 La Garenne-Colombes cedex, France

ARTICLE INFO

Article history:
Received 1 August 2015
Received in revised form
5 October 2015
Accepted 7 October 2015
Available online 13 October 2015

Keywords:
EBSD
Aluminium alloys
Casting
Fatigue
SDAS
Defect

ABSTRACT

This paper is dedicated to the high cycle fatigue (HCF) behaviour of cast Al–Si alloys. In particular, three similar alloys with different microstructural characteristics are investigated. The result of an experimental campaign is presented, in order to characterise the fatigue behaviour, and more specifically the fatigue damage mechanisms related to the different microstructural heterogeneities (i.e. casting porosity, dendrite size, SDAS, non-metallic inclusions and silicon particles), observed under different multiaxial loading conditions: pure tension, plane bending, pure torsion and combined tension–torsion with a load ratio $R=-1$.

It is shown that casting porosity has a very detrimental influence on the uniaxial and combined tension–torsion fatigue strengths. However, a much lower influence is observed for the torsional fatigue strength.

For the porosity-free alloy, it is observed that the formation of persistent slip bands (PSB) in the aluminium matrix is the major fatigue crack initiation mechanism regardless of the loading modes, at a load ratio of $R=-1$. It is also shown that the aluminium matrix has a large role in the formation of PSB and that the Si particles facilitate the formation of PSB.

1. Introduction

Automotive manufacturers have the choice of several casting processes and post-casting heat treatments for the fabrication of cast aluminium components, such as cylinder heads, used in their vehicles. Typical casting processes include gravity die casting and lost foam casting (LFC) and the components are subsequently heat treated via standard T6 or T7 treatments and/or the HIP treatment. Each casting process and heat treatment combination has certain advantages and disadvantages. From a material point of view, each casting process-post casting treatment combination results in a different microstructure, which can be characterised by the following microstructural features:

- casting defect, notably micro-shrinkage pores and gas porosity;
- the aluminium matrix, often characterised by the DAS (dendrite arm spacing), the SDAS (secondary dendrite arm spacing) and the precipitation hardening level;
- inclusions, in particular silicon particles in the eutectic zones and intermetallics.

The influence of these factors on the HCF behaviour of these materials has been investigated by many researchers. The effect of casting porosity has been studied by [1–4] and the effect of the microstructure (i.e. the aluminium matrix and the silicon particles) by [5–7]. However, these studies are often limited to uniaxial fatigue behaviour.

The principal aim of this work is to investigate the influence of different microstructural heterogeneities found in cast aluminium–silicon alloys on the HCF behaviour for different loading modes. Specifically, the fatigue damage mechanisms associated with the microstructural features discussed above are investigated. In order to achieve this aim, an extensive multiaxial HCF testing campaign was conducted, including uniaxial tension–compression loads, pure torsion and combined tension–torsion, on three different Al–Si alloys. These alloys were fabricated by three different processes and therefore they have significantly different microstructures, particularly in terms of their casting defect populations.

* Corresponding author at: Arts et Métiers ParisTech, CER Angers – Laboratoire LAMPA – 2 Bd du Ronceray, 49035 Angers Cedex 1, France. Fax: +33 242207320.
E-mail address: viet-duc.le@ensam.eu (V.-D. Le).

http://dx.doi.org/10.1016/j.msea.2015.10.026
0921-5093/

2. Cast aluminium alloys under investigation

Fig. 1 shows typical microstructural images of the aluminium alloys under investigation which highlight the different microstructural heterogeneities discussed above.

2.1. Manufacturing processes for the three investigated alloys

The three cast aluminium alloys investigated in this study, referred as alloys A, B and C, were elaborated by either gravity die casting or lost foam casting and then were subjected to either a standard T7 heat treatment or a Hot Isostatique Pressing (HIP) followed by a T7 treatment (see Table 1).

Alloy A corresponds to the gravity die cast material introduced in the work of Koutiri et al. [1]. This material is cast by PSA Peugeot–Citroen in the form of cylinder heads using their industrial production process, however certain modification was made in order to have a much larger volume of material from which fatigue specimens could be extracted. This was done be reducing the length of the inlet and exhaust cores (Fig. 2a). The resulting modified cylinder heads have blocked inlet and exhaust passages on the engine block mating surface (Fig. 2b). This resulted in layer of material with a maximum thickness of 10 mm from which the specimens (Fig. 7) can be extracted.

Lost foam casting is used to fabricate alloys B and C and the material is cast in the form of plates, 200 mm × 150 mm × 18 mm in size. This leads to a material with a high porosity volume fraction. Consequently, it should be noted that the microstructure and the defect size distribution of alloys B and C are not representative of the material present in industrially cast cylinder heads.

The two post-casting heat treatments are presented below:

- *HIP treatment*: tempering at a temperature of approximately 500 °C under a pressure of approximately 1000 bars.
- *T7 heat treatment*:
  - Solution heat-treatment for 5 h at a temperature of 535–540 °C.
  - Water quenching at a temperature of 60–70 °C.
  - Tempering at 200 °C for 5–5.5 h.
  - Cooling in ambient air.

Table 1 lists the chemical compositions, casting processes and heat treatments for each of the investigated materials.

2.2. Microstructure characterisation and monotonic mechanical properties

2.2.1. The aluminium matrix

The primary alpha matrix is typically characterised by the Secondary Dendrite Arm Spacing (SDAS). This quantity is determined by identifying individual aluminium dendrites, the SDAS is then measured as the distance between the secondary dendrite arms (Fig. 3(a)). Forty dendrites of each material were measured and the SDAS distributions of the three materials are shown in Fig. 3(b). It can be seen that the SDAS of alloy A ($SDAS_A = 42.3 \pm 9.7\ \mu m$) is the smallest while that of material B ($SDAS_B = 77.3 \pm 18.9\ \mu m$) and C ($SDAS_C = 91.4 \pm 32.8\ \mu m$) are larger. For the casting of aluminium alloys the SDAS is inversely proportional to solidification rate [5]. As such the difference in the SDAS between alloys A and B/C can be explained by the fact that the solidification rate in gravity die casting in which metallic moulds are used (for alloy A) is greater than that in lost foam sand casting (alloys B and C).

As regard to the dendrite size, EBSD measurements have been conducted to characterise the distribution of the dendrite size. Three samples of alloys A and C with the same geometry as the fatigue specimens (Fig. 7(a)), but with a flat zone on the cylindrical section (see Fig. 7(b)), were prepared. The surface was firstly mechanically polished and then electrochemically etched using a 20:80 (%volume) HNO3/CH4Co solution at 0–5 °C and 15 V for 10 s. The spatial resolution of EBSD measurements is 5 μm × 5 μm. Fig. 4 shows an EBSD inverse pole figure cartography.

Using the data obtained by EBSD measurements, the grain size distributions are determined (Fig. 5). Note that these distributions are not based on the percentage of the number of grains but on the grain area percentage. The average grain size $D_{e,average}$ is then determined by the following equation [8]:

$$D_{e,average} = \Sigma_i (D_{e_i} . f_i) \tag{1}$$

where $D_{e,i}$ is the equivalent diameter of grain i calculated from the area of grain i, $area_i$, by Eq. (2), and f_i is the grain size percentage of grain i

$$D_{e,i} = \sqrt{\frac{4 \times area_i}{\pi}} \tag{2}$$

The average grain size of alloy A (337 μ m) is smaller than that of alloy C (464 μm). This difference is in agreement with the results obtained for the SDAS of these two alloys (Fig. 3(b)).

In addition, the micro-hardnesses of the alpha phase of the

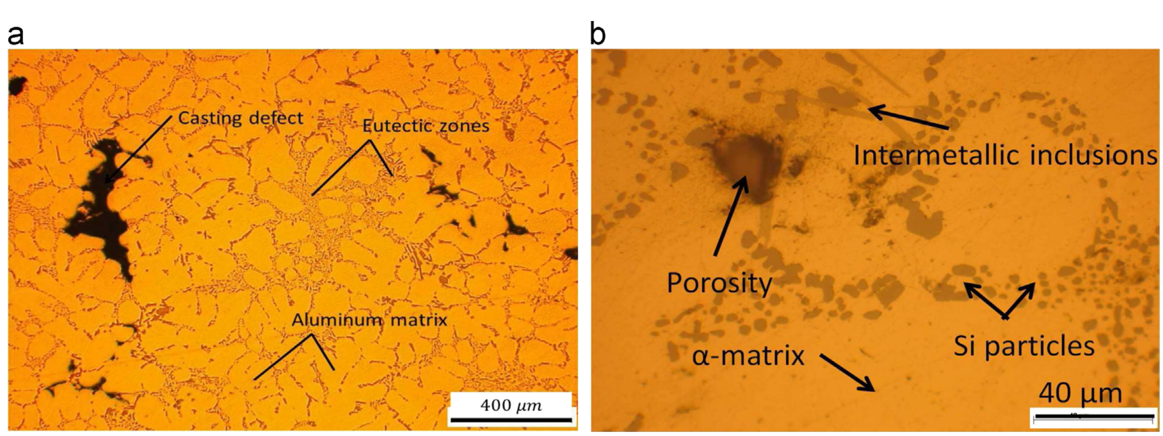

Fig. 1. Microstructural heterogeneities present in the cast aluminium alloys under investigation: (a) typical microstructure of cast aluminium alloys; (b) zoomed view.